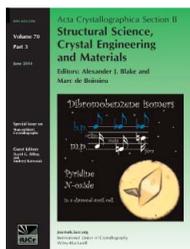# *In-situ* high-pressure powder X-ray diffraction study of α-zirconium phosphate

Jennifer E. Readman, Alistair Lennie and Joseph A. Hriljac

Crystallography Journals Online is available from **journals.iucr.org**

In-situ high-pressure powder X-ray diffraction study of α-zirconium phosphate

Jennifer E. Readman,[a] Alistair Lennie[b] and Joseph A. Hriljac[c]*

[a]Centre for Materials Science, University of Central Lancashire, Preston, Lancashire PR1 2HE, England, [b]Synchrotron Radiation Source, Daresbury Laboratory, Warrington WA4 4AD England, and [c]School of Chemisty, University of Birmingham, Birmingham B15 2TT, England

Correspondence e-mail: j.a.hriljac@bham.ac.uk

The high-pressure structural chemistry of α-zirconium phosphate, α-$Zr(HPO_4)_2 \cdot H_2O$, was studied using *in-situ* high-pressure diffraction and synchrotron radiation. The layered phosphate was studied under both hydrostatic and non-hydrostatic conditions and Rietveld refinement carried out on the resulting diffraction patterns. It was found that under hydrostatic conditions no uptake of additional water molecules from the pressure-transmitting medium occurred, contrary to what had previously been observed with some zeolite materials and a layered titanium phosphate. Under hydrostatic conditions the sample remained crystalline up to 10 GPa, but under non-hydrostatic conditions the sample amorphized between 7.3 and 9.5 GPa. The calculated bulk modulus, $K_0 = 15.2$ GPa, showed the material to be very compressible with the weak linkages in the structure of the type Zr—O—P.

1. Introduction

The high-pressure structural chemistry of zeolites and related framework materials has been extensively studied (Hriljac, 2006; Gatta, 2008; Chapman *et al.*, 2008; Bennett *et al.*, 2011) and several interesting phenomena such as pressure-induced expansion and superhydration have been reported. It was first noted in the early 1980s that the volume compressibility of zeolite Na-A changed depending on the pressure-transmitting medium used (Hazen, 1983; Hazen & Finger, 1984). This work was later followed up by Hriljac and co-workers who also investigated different cation-exchanged forms of zeolite-A including Ca-A and Zn-A (Hriljac, 2006). It was found that the nature of the charge-balancing cation played an important role in high-pressure structural chemistry; for Zn-A a large reversible increase in the unit-cell parameter occurred when the pressure-transmitting medium contained water but not for Ca-A. It was speculated that the water molecules had gone into the pores of the zeolite resulting in pressure-induced expansion. This phenomena had also been observed in natrolite-type zeolites (Lee *et al.*, 2001, 2002, 2006, 2011; Colligan *et al.*, 2004) and the $ANbWO_6$ defect pyrochlore (where A = Rb^+ or NH_4^+; Barnes *et al.*, 2003; Perottoni & da Jornada, 1997). However, these materials are three-dimensional structures, whereas little work has been carried out on two-dimensional layered materials. There have been reports of certain graphite oxide intercalation compounds forming under high pressure (Talyzin *et al.*, 2009) and also the pressure-induced uptake of water molecules into the interlayer spacings of clay materials such as Na-hectorite (You *et al.*,

2013). The high-pressure chemistry of a layered pentylamine intercalated lepidocrocite-type titanate, $(C_5H_{11}NH_3)_{0.5}$-$H_{0.3}Ni_{0.4}Ti_{1.6}O_4 \cdot nH_2O$, was studied by Nakano *et al.* (1998) using *in-situ* high-pressure powder diffraction. Under hydrostatic conditions using either methanol or ethanol as the pressure medium, a discontinuity in the interlayer spacing was observed indicating that the material had taken up the alcohol.

Another family of layered materials are the metal(IV) phosphates. The most familiar of these is α-zirconium phosphate, $Zr(HPO_4)_2 \cdot H_2O$. The ion-exchange and intercalation properties of this material have been extensively studied (Alberti, 1978; Clearfield & Costantino, 1996). A wide range of monovalent and divalent cations have been shown to exchange into α-zirconium phosphate. Unlike traditional clay-like materials, α-zirconium phosphate does not swell in water and has been shown to be more stable thermally. However, amines, alkanols and glycols have been intercalated into the layers (Costantino, 1979) as well as larger molecules such as aminomethylcrowns (Yamamoto *et al.*, 1998). A metastable superhydrated form, θ-zirconium phosphate, exists which contains eight water molecules between the layers as opposed to the one in α-zirconium phosphate (Clearfield *et al.*, 1973), but due to the unstable nature of the material no structural characterization has been carried out. Both the intercalation chemistry of the α-phase and presence of the θ-phase suggest

water might be forced in under high pressure in a similar fashion to the zeolites or lepidocrocite-type titanate. The work here presents an *in-situ* high-pressure powder X-ray diffraction study of α-zirconium phosphate to test this and also to see how the structure itself changes with pressure.
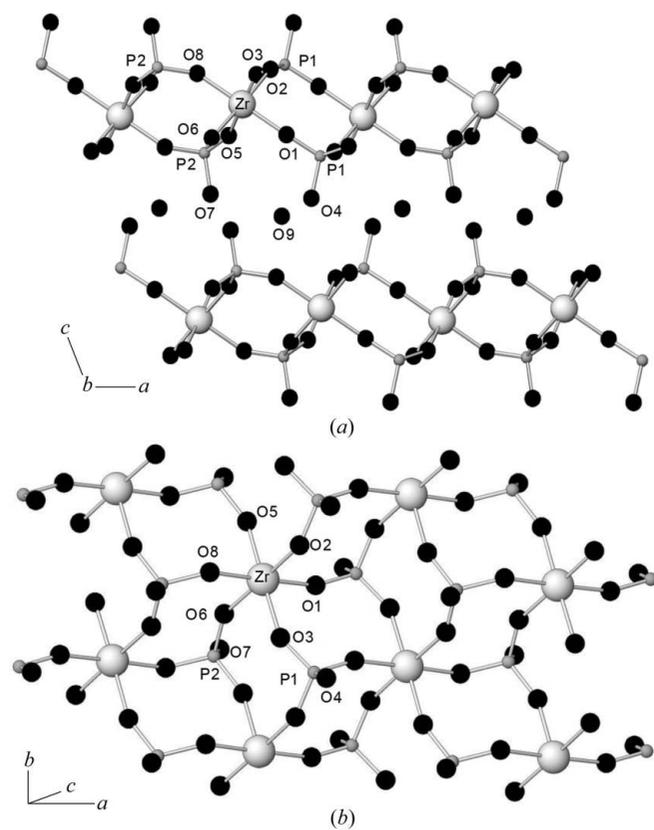
The structure of α-zirconium phosphate was reported by Troup & Clearfield (1977) by single-crystal X-ray diffraction. The material was found to be monoclinic, space group $P2_1/n$ with $a = 9.060$ (2), $b = 5.297$ (1), $c = 15.414$ (3) Å and $\beta = 101.71$ (2)°. The structure consists of layers of vertex-sharing octahedral zirconium and tetrahedral phosphorus with water molecules located between the layers, as shown in Fig. 1.

2. Experimental

Crystalline α-zirconium phosphate was prepared using hydrothermal methods. A poorly crystalline sample was first prepared by co-precipitation of 1.25 *M* H_3PO_4 (Fisher) with 1.7 *M* $ZrOCl_2$ [30% wt in HCl (Aldrich)] according to the preparation of Trobajo *et al.* (2000). The resulting product was washed with 0.3 *M* H_3PO_4 and centrifuged to remove excess liquid. To produce a crystalline sample, 10 g of poorly crystalline material was then placed in a stainless steel autoclave with 25 ml of 12 *M* H_3PO_4 and heated at 423 K for 4 d. The product was then washed with 0.3 *M* H_3PO_4, centrifuged and dried under ambient conditions. A diffraction pattern of the sample was obtained prior to the high-pressure work, and a Rietveld refinement confirmed the purity and the refined unit cell and atomic positions matched well to the reported crystal structure. The fit is included in the supporting information.[1]

In-situ diffraction experiments were carried out at Station 9.5 HPT at the Synchrotron Radiation Source, Daresbury Laboratory, England, using a wavelength of 0.444 Å. The sample was packed in a 150 μm diameter hole in a stainless steel diamond–anvil cell gasket with ruby chips and a 16:3:1 mixture of methanol, ethanol and water to preserve hydrostatic conditions; 700 μm culet Boehler–Almax diamonds were used. A MAR345 image-plate detector was used with 300 s exposure times at each pressure, the normalized diffraction patterns were obtained by integrating over the whole plate using the program *FIT2D* (Hammersley *et al.*, 1996). Sample pressures were determined by the standard technique of detecting the shift in the R1 emission line of included ruby chips and are estimated to be accurate to *ca* 0.1 GPa (Mao *et al.*, 1986). Data were collected at intervals up to a pressure of approximately 10 GPa and then the pressure was slowly released to ambient. A second pressure run was carried out using a fresh sample of α-zirconium phosphate which was loaded into the diamond–anvil cell dry. Data were collected at intervals up to a pressure of approximately 9.5 GPa, at which pressure the crystallinity of the sample had degraded considerably. An ambient pressure diffraction pattern was collected *ex-situ*.

Figure 1
Schematic representation of the structure of α-zirconium phosphate. (*a*) The stacking of the zirconium phosphate layers. Light grey, dark grey and black represent zirconium, phosphorus and oxygen, respectively. (*b*) Along the *ab* plane showing the octahedral zirconium and tetrahedral phosphorus coordination.

[1] Supporting information for this paper is available from the IUCr electronic archives (Reference: ZB5035).

Table 1
Variation in unit-cell volume and lattice parameters with pressure for α-zirconium phosphate under hydrostatic conditions.

Pressure (GPa)	a (Å)	b (Å)	c (Å)	β (°)	V (Å³)
0.0001†	9.0520 (1)	5.2842 (1)	15.4189 (3)	101.713 (1)	722.17 (2)
0.71	8.9526 (2)	5.2243 (1)	15.0834 (1)	101.556 (4)	691.17 (6)
1.40	8.8958 (3)	5.1915 (2)	14.9405 (1)	101.524 (6)	676.08 (8)
1.98	8.8337 (4)	5.1573 (3)	14.7855 (18)	101.40 (10)	660.15 (9)
2.53	8.7799 (2)	5.1301 (1)	14.6698 (9)	101.473 (5)	647.34 (5)
3.23	8.7287 (3)	5.1039 (2)	14.5503 (12)	101.469 (6)	635.28 (6)
5.60	8.5769 (3)	5.0263 (2)	14.2388 (10)	101.502 (5)	601.51 (5)
6.35	8.5259 (3)	4.9993 (2)	14.1508 (11)	101.486 (6)	591.08 (6)
6.77	8.5100 (3)	4.9909 (2)	14.1225 (10)	101.472 (5)	587.83 (5)
8.88	8.4115 (3)	4.9372 (2)	13.9691 (11)	101.398 (6)	568.69 (5)
10.04	8.3593 (4)	4.9123 (2)	13.8705 (15)	101.296 (9)	558.54 (7)
7.39	8.4657 (3)	4.9706 (2)	14.0465 (13)	101.407 (7)	579.39 (6)
4.92	8.5996 (4)	5.0418 (2)	14.2879 (14)	101.436 (7)	607.19 (4)
4.00	8.6660 (4)	5.0757 (2)	14.4259 (13)	101.405 (8)	622.01 (7)
3.23	8.7120 (4)	5.0986 (2)	14.5269 (14)	101.377 (9)	632.59 (7)
0.30	8.9976 (7)	5.2512 (4)	14.2472 (21)	101.551 (9)	705.82 (12)
0.0001‡	9.0469 (4)	5.2862 (3)	15.4312 (20)	101.597 (7)	722.91 (11)

† *Ex-situ* measurement before pressure run. ‡ *In-situ* measurement after pressure run.

Table 2
Refinement statistics obtained from Rietveld refinement of hydrostatic pressure data.

Pressure (GPa)	R_p	R_{wp}	R_{F^2}
0.0001†	0.010	0.013	0.039
0.71	0.006	0.008	0.112
1.40	0.008	0.011	0.156
1.98	0.011	0.014	0.152
2.53	0.006	0.008	0.073
3.23	0.006	0.007	0.098
5.60	0.006	0.009	0.078
6.35	0.007	0.009	0.080
6.77	0.006	0.008	0.059
8.88	0.006	0.009	0.113
10.04	0.008	0.012	0.140
7.39	0.007	0.009	0.117
4.92	0.008	0.011	0.170
4.00	0.007	0.010	0.096
3.23	0.007	0.010	0.108
0.30	0.009	0.013	0.183
0.0001‡	0.007	0.010	0.126

† *Ex-situ* measurement before pressure run. ‡ *In-situ* measurement after pressure run.

Analysis of the diffraction data was carried out using the *GSAS* suite of programs and the *EXPGUI* interface (Toby, 2001; Larson & Von Dreele, 2004). Rietveld refinement was carried out in the following manner. After defining the background points and refinement of the scale factor, the lattice parameters were allowed to vary, followed by initial refinement of the peak-profile coefficients. Next, atomic coordinates were refined, followed by isotropic displacement parameters. The P—O distances were constrained to be approximately 1.5 Å using soft constraints of 0.1 Å; this was sufficient to keep the distances in a reasonable range but not so constrained to force an unrealistically short P—OH distance. The quoted estimated standard uncertainties are as determined from the Rietveld refinements and not corrected

for well known underestimation due to data correlations (Bérar & Lelann, 1991) and the use of image-plate data. A conservative estimate of their underestimation is a factor of 3. The *EOSfit* program (Angel, 2000) was used to calculate the bulk modulus using a third-order Birch–Murnaghan equation of state.

3. Results and discussion

3.1. Hydrostatic conditions

Examination of the diffraction patterns (Fig. 2) indicated that no phase changes had taken place in the pressure range studied and this was later confirmed by Rietveld analysis as all patterns could be refined in the space group $P2_1/n$, as reported by Troup & Clearfield (1977). Likewise, over the pressure range studied the sample remained highly crystalline as the diffraction peaks remained sharp. Difference Fourier maps were used to check for the additional water molecules that would indicate superhydration, but no residual electron density attributable to extra water molecules was present and all patterns were well fit without the need for adding extra water molecules.

The results from the Rietveld refinements show there is a smooth decrease in unit-cell volume with increasing pressure
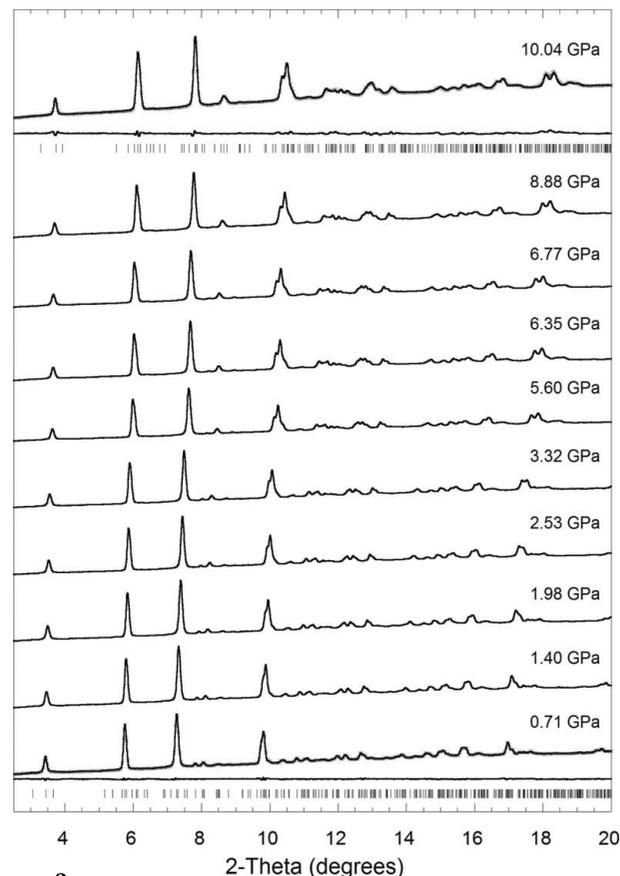
Figure 2
Observed patterns for α-zirconium phosphate under hydrostatic conditions up to 10.04 GPa; the lowest and highest pressure patterns include results from the Rietveld fits with difference plots and reflection markers below the patterns.

and no evidence of a volume expansion that would be indicative of pressure-induced hydration (Table 1). The fits are of high quality for all pressures (Table 2) even up to 10 GPa. Plots of the observed, calculated and difference plots for all pressures and the CIF file for the 10.04 GPa fit are presented in the supporting information. Over the pressure range studied this compression is completely reversible with no hysteresis in unit-cell parameters, as shown in Fig. 3.

In the Rietveld refinements the only restraints used were that the phosphorus–oxygen distances should be approximately 1.5 Å. Therefore, the zirconium–oxygen distances were allowed to vary freely and also all bond angles were unconstrained. Assuming the PO_4 tetrahedra are quite rigid, then a possible mechanism for compression would be to introduce strain in the zirconium–oxygen–phosphorus linkages. Details of the zirconium–oxygen bond distances and zirconium–

oxygen–phosphorus bond angles are given in Tables 3 and 4, respectively. None of the six zirconium–oxygen bond distances show strong and consistent changes with increasing pressure, those to atoms O1, O5, O6 and O8 are within 3 standard uncertainties of each other and vary from 1.95 to 2.18 Å. Distances to O2 and O3 are generally longer, in particular the Zr—O3 distances at the highest pressures, and this holds upon decompression. Both of these O atoms are bonded to P1 and are adjacent to each other in the ZrO_6 octahedra. In general, all six of the Zr—O—P bond angles either remain the same with increasing pressure (O2, O5 and O8) or show a decrease. Plots displaying the representative variation of the Zr—O3—P1 and Zr—O6—P2 angles are shown in Figs. 4 and 5, respectively. As there is no significant decrease in bond distances, we can therefore conclude that the compression mechanism involves rigid PO_4 tetrahedra and mostly rigid ZrO_6 octahedra which move closer together by bending the bridging O atoms.

Determination of the bulk modulus was carried out by using a Birch–Murnaghan equation of state with three parameters. V_0 was found to be 721.94 Å^3, K_0 = 15.2 GPa and K' = 7.9. The
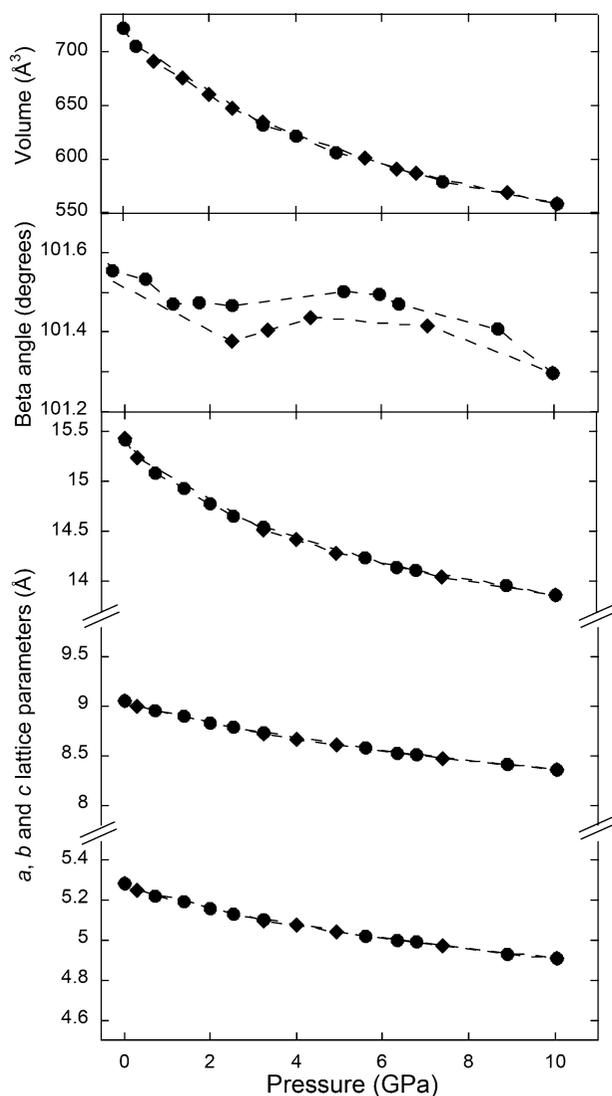
Figure 3
Plot showing variations in the *a*-axis, *b*-axis, *c*-axis, β angle and unit-cell volume parameters (bottom to top, respectively) with pressure under hydrostatic conditions. The circles represent increasing pressure and the diamonds decreasing pressure. Estimated standard uncertainties are smaller than the symbols.
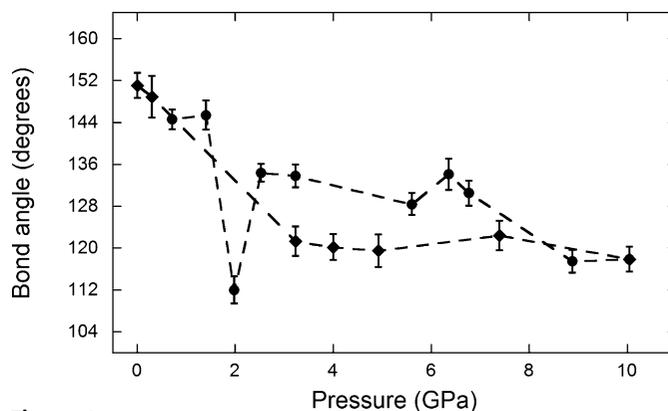
Figure 4
Plot showing variation in the Zr—O3—P1 bond angle with pressure under hydrostatic conditions. The circles represent increasing pressure and the diamonds decreasing pressure.
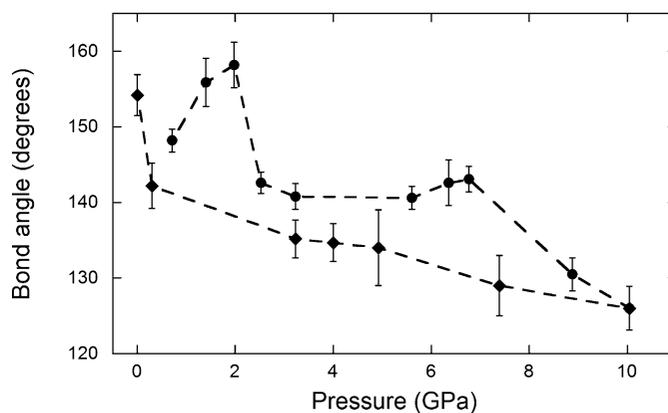
Figure 5
Plot showing variation in the Zr—O6—P2 bond angle with pressure under hydrostatic conditions. The circles represent increasing pressure and the diamonds decreasing pressure.

Jennifer E. Readman *et al.* · *In-situ* high-pressure diffraction **513**

Table 3
Zirconium–oxygen bond distances obtained from Rietveld refinement of hydrostatic data.

Pressure (GPa)	Zr—O1 (Å)	Zr—O2 (Å)	Zr—O3 (Å)	Zr—O5 (Å)	Zr—O6 (Å)	Zr—O8 (Å)
0.0001†	2.078 (8)	2.073 (12)	2.097 (13)	2.107 (12)	2.122 (12)	2.081 (7)
0.71	2.02 (2)	2.09 (3)	2.12 (3)	2.14 (2)	2.09 (2)	2.13 (2)
1.40	1.99 (2)	2.14 (4)	2.07 (3)	2.08 (3)	1.94 (3)	2.15 (3)
1.98	1.97 (3)	2.11 (4)	2.57 (3)	2.00 (3)	1.95 (3)	2.18 (4)
2.53	2.04 (2)	2.19 (2)	2.14 (2)	2.12 (2)	2.01 (2)	2.08 (2)
3.23	2.03 (3)	2.21 (3)	2.15 (3)	2.10 (3)	2.03 (3)	2.04 (3)
5.60	2.09 (3)	2.14 (3)	2.19 (3)	2.05 (3)	2.08 (2)	2.01 (2)
6.35	2.05 (4)	2.29 (3)	2.12 (4)	2.18 (4)	2.03 (3)	2.06 (4)
6.77	2.05 (3)	2.27 (3)	2.16 (4)	2.07 (4)	1.99 (3)	2.04 (3)
8.88	2.03 (4)	2.14 (5)	2.33 (3)	2.00 (3)	2.07 (4)	2.07 (4)
10.04	2.06 (4)	2.00 (4)	2.37 (3)	1.97 (3)	2.10 (4)	2.21 (4)
7.39	2.03 (5)	2.08 (6)	2.30 (3)	2.02 (3)	2.11 (6)	2.08 (5)
4.92	1.99 (6)	2.08 (6)	2.36 (4)	2.03 (3)	2.10 (6)	2.07 (6)
4.00	1.99 (4)	2.14 (4)	2.37 (3)	2.06 (3)	2.10 (4)	2.06 (4)
3.23	1.99 (4)	2.11 (4)	2.38 (3)	2.06 (3)	2.08 (4)	2.04 (4)
0.30	2.04 (3)	2.52 (3)	2.03 (3)	2.00 (3)	2.03 (4)	2.06 (3)
0.0001‡	2.11 (2)	2.19 (3)	2.04 (3)	2.10 (3)	2.072 (3)	2.13 (2)

† *Ex-situ* measurement before pressure run.   ‡ *In-situ* measurement after pressure run.

Table 4
Zirconium–oxygen–phosphorus bond angles obtained from Rietveld refinement of hydrostatic data.

Pressure (GPa)	Zr—O1—P1 (°)	Zr—O2—P1 (°)	Zr—O3—P1 (°)	Zr—O5—P2 (°)	Zr—O6—P2 (°)	Zr—O8—P2 (°)
0.0001†	160.1 (9)	144.5 (8)	147.5 (8)	157.9 (9)	149.4 (7)	144.8 (7)
0.71	159 (2)	143 (2)	145 (2)	135 (2)	148 (2)	136 (2)
1.40	159 (3)	141 (3)	145 (3)	155 (3)	156 (3)	138 (3)
1.98	152 (3)	131 (3)	112 (2)	141 (3)	158 (3)	128 (3)
2.53	149 (2)	131 (2)	134 (2)	137 (2)	143 (1)	137 (2)
3.23	145 (3)	130 (2)	134 (2)	135 (2)	141 (2)	137 (3)
5.60	134 (2)	134 (2)	128 (2)	136 (2)	141 (2)	143 (2)
6.35	140 (3)	122 (2)	134 (3)	127 (3)	143 (3)	133 (3)
6.77	141 (2)	122 (2)	131 (3)	133 (2)	143 (2)	132 (3)
8.88	135 (3)	132 (3)	118 (2)	137 (2)	131 (2)	132 (3)
10.04	131 (2)	143 (3)	119 (2)	136 (2)	126 (3)	124 (3)
7.39	137 (3)	134 (4)	122 (2)	136 (3)	129 (4)	132 (4)
4.92	140 (5)	135 (5)	120 (2)	141 (3)	134 (5)	138 (5)
4.00	145 (3)	136 (3)	120 (2)	141 (3)	135 (3)	137 (3)
3.23	143 (3)	138 (3)	121 (2)	142 (3)	135 (3)	139 (3)
0.30	158 (4)	116 (2)	149 (3)	158 (4)	142 (3)	147 (3)
0.0001‡	156 (2)	126 (2)	151 (3)	153 (2)	154 (3)	147 (2)

† *Ex-situ* measurement before pressure run.   ‡ *In-situ* measurement after pressure run.

Table 5
Parameters obtained from fitting of the unit-cell data under both hydrostatic and non-hydrostatic conditions to obtain the bulk moduli.

	Hydrostatic		Non-hydrostatic	
	K_0 (GPa)	K_0'	K_0 (GPa)	K_0'
Volume	15.2	7.9	19.0	3.9
a	21.5	5.7	22.7	5.5
b	23.0	6.6	11.4	26
c	6.83	11	13.4	2.4

low value of K_0 indicates the material is very compressible as expected. There have been few reports of the compressibility of other phosphate materials. Zhai *et al.* (2011) studied strontium orthophosphate, $Sr_3(PO_4)_2$, which is a dense phosphate, at pressures up to 20.0 GPa and found K_0 to be 89.5 (17) GPa. As previously mentioned, little work of this nature has been carried out on layered materials, so there are few comparisons to be made. However, talc, which is a layered magnesium silicate, has an experimental K_0 value of 41.6 (9) GPa (Stixrude, 2002), which is considerably higher than that of *α*-zirconium phosphate presented here. Values of the compressibility along each unit-cell axis were also determined using *EOSfit*. Details of the parameters obtained are given in Table 5. As expected, the *c* parameter is considerably more compressible than either *a* or *b* as this is the crystallographic direction perpendicular to the layers.

3.2. Non-hydrostatic conditions

All diffraction data (Fig. 6) could be analysed in the space group $P2_1/n$ up to a pressure of 7.33 GPa. Data collected after this pressure were of low quality due to a significant loss of crystallinity which persisted upon pressure release. The resulting refined unit-cell parameters are given in Table 6. The errors associated with these parameters are approximately 4–5 times larger than those under hydrostatic conditions (Table 1); this is due to peak broadening resulting in considerable overlap at higher 2θ values. As a consequence of this, atomic positions and displacement parameters were not refined. All Rietveld fits are presented in the supporting information.

The unit-cell parameters were used to obtain the equation of state parameters. Again a three-term Birch–Murnaghan equation was used and gave V_0 to be 730.98 Å^3, K_0 = 19.0 GPa and K' = 3.9. The value of the non-hydrostatic bulk modulus is almost 4 GPa higher than that calculated from the hydrostatic data. This is consistent with the findings of Bassett (2006). Where there is little or no pressure medium deviatoric stress can occur. The X-ray beam passes through one diamond, the sample and then exits through the other diamond, hence passing along the direction of most stress. As a result the *d*-spacings sampled may be shifted to lower 2θ resulting in larger unit-cell volumes. Larger unit-cell volumes will therefore result in a seemingly less compressible material.

4. Conclusion

High-pressure *in-situ* powder X-ray diffraction of layered *α*-zirconium phosphate indicates that no phase changes (*e.g.* to

Table 6
Variation in unit-cell parameters and volume with pressure for α-zirconium phosphate under non-hydrostatic conditions.

| Pressure (GPa)	a (Å)	b (Å)	c (Å)	β (°)	V (Å³)
0.140	9.0581 (3)	5.2855 (2)	15.4388 (13)	101.733 (4)	723.71 (7)
0.30	9.0234 (13)	5.2808 (7)	15.401 (4)	101.51 (2)	719.1 (2)
0.85	8.9597 (14)	5.2515 (7)	15.134 (3)	101.34 (2)	701.0 (2)
2.12	8.8454 (12)	5.1792 (7)	14.819 (4)	101.34 (2)	665.6 (2)
2.67	8.8122 (10)	5.1598 (6)	14.728 (4)	101.32 (2)	656.7 (2)
3.37	8.7600 (10)	5.1350 (6)	14.574 (4)	101.33 (2)	642.8 (2)
4.51	8.6599 (14)	5.0938 (8)	14.225 (5)	101.31 (4)	615.3 (3)
5.48	8.5966 (19)	5.0744 (10)	13.970 (8)	101.33 (6)	597.5 (4)
5.76	8.576 (2)	5.0668 (11)	13.876 (9)	101.31 (7)	591.2 (4)
6.91	8.544 (2)	5.0541 (11)	13.771 (9)	101.27 (7)	583.2 (5)
7.33	8.522 (2)	5.0446 (12)	13.715 (10)	101.25 (8)	578.3 (5)

produce the θ-form) or phenomena such as pressure-induced expansion or superhydration take place when using a mixture of methanol, ethanol and water as the pressure-transmitting fluid. This is in contrast to many zeolites and the few reports of

related layered silicates. Under hydrostatic conditions up to 10 GPa all powder data could be refined using the Rietveld method in the $P2_1/n$ space group. Examination of the bond distances and angles suggested that the compression mechanism involved deformation of the $Zr-O-P$ linkages and in particular the $Zr-O3-P1$ and $Zr-O6-P1$ linkages. The refined unit-cell volumes could be fitted using a three-term Birch–Murnaghan equation of state and the resulting bulk modulus of 15.2 GPa indicates the material is very compressible. Examination of the compressibilities shows this is principally due to contraction along the c-axis perpendicular to the metal phosphate layers. Under non-hydrostatic conditions, the solid compresses in a similar fashion up to 7.3 GPa but then amorphizes if the pressure is further increased.

Figure 6
Observed diffraction patterns for α-zirconium phosphate under non-hydrostatic conditions.

References

Alberti, G. (1978). *Acc. Chem. Res.* **11**, 163–170.
Angel, R. J. (2000). *Rev. Mineral. Geochem.* **41**, 35–59.
Barnes, P. W., Woodward, P. M., Lee, Y., Vogt, T. & Hriljac, J. A. (2003). *J. Am. Chem. Soc.* **125**, 4572–4579.
Bassett, W. A. (2006). *J. Phys. Condens. Matter*, **18**, S921–S931.
Bennett, T. D., Simoncic, P., Moggach, S. A., Gozzo, F., Macchi, P., Keen, D. A., Tan, J. & Cheetham, A. K. (2011). *Chem. Commun.* **47**, 7983–7985.
Bérar, J.-F. & Lelann, P. (1991). *J. Appl. Cryst.* **24**, 1–5.
Chapman, K. W., Halder, G. J. & Chupas, P. J. (2008). *J. Am. Chem. Soc.* **130**, 10524–10526.
Clearfield, A. & Costantino, U. (1996). *Comprehensive Supramolecular Chemistry*, Vol. 17, p. 107. Oxford: Pergamon Press.
Clearfield, A., Landis, A. L., Medina, A. S. & Troup, J. H. (1973). *J. Inorg. Nucl. Chem.* **35**, 1099–1108.
Colligan, M., Forster, P. M., Cheetham, A. K., Lee, Y., Vogt, T. & Hriljac, J. A. (2004). *J. Am. Chem. Soc.* **126**, 12015–12022.
Costantino, U. (1979). *J. Chem. Soc. Dalton Trans.* pp. 402–405.
Gatta, G. D. (2008). *Z. Kristallogr.* **223**, 160–170.
Hammersley, A. P., Svensson, S. O., Hanfland, M., Fitch, A. N. & Hausermann, D. (1996). *High Pressure Res.* **14**, 235–248.
Hazen, R. M. (1983). *Science*, **219**, 1065–1067.
Hazen, R. M. & Finger, L. W. (1984). *J. Appl. Phys.* **56**, 1838–1840.
Hriljac, J. A. (2006). *Crystallogr. Rev.* **12**, 181–193.
Larson, A. C. & Von Dreele, R. B. (2004). *GSAS*. Report LAUR 86–748. Los Alamos National Laboratory, New Mexico, USA.
Lee, Y., Hriljac, J. A., Parise, J. B. & Vogt, T. (2006). *Am. Mineral.* **91**, 247–251.
Lee, Y., Hriljac, J. A., Vogt, T., Parise, J. B. & Artioli, G. (2001). *J. Am. Chem. Soc.* **123**, 12732–12733.
Lee, Y., Seoung, D., Liu, D., Park, M. B., Hong, S. B., Chen, H., Bai, J., Kao, C., Vogt, T. & Lee, Y. (2011). *Am. Mineral.* **96**, 393–401.
Lee, Y., Vogt, T., Hriljac, J. A., Parise, J. B. & Artioli, G. (2002). *J. Am. Chem. Soc.* **124**, 5466–5475.
Mao, H. K., Xu, J. & Bell, P. M. (1986). *J. Geophys. Res. B Solid Earth Planets*, **91**, 4673–4676.
Nakano, S., Sasaki, T., Takemura, K. & Watanabe, M. (1998). *Chem. Mater.* **10**, 2044–2046.
Perottoni, C. & da Jornada, J. (1997). *Phys. Rev. Lett.* **78**, 2991–2994.
Stixrude, L. (2002). *J. Geophys. Res.* **107**, 2327–2336.
Talyzin, A. V., Sundqvist, B., Szabó, T., Dékány, I. & Dmitriev, V. (2009). *J. Am. Chem. Soc.* **131**, 18445–18449.
Toby, B. H. (2001). *J. Appl. Cryst.* **34**, 210–213.
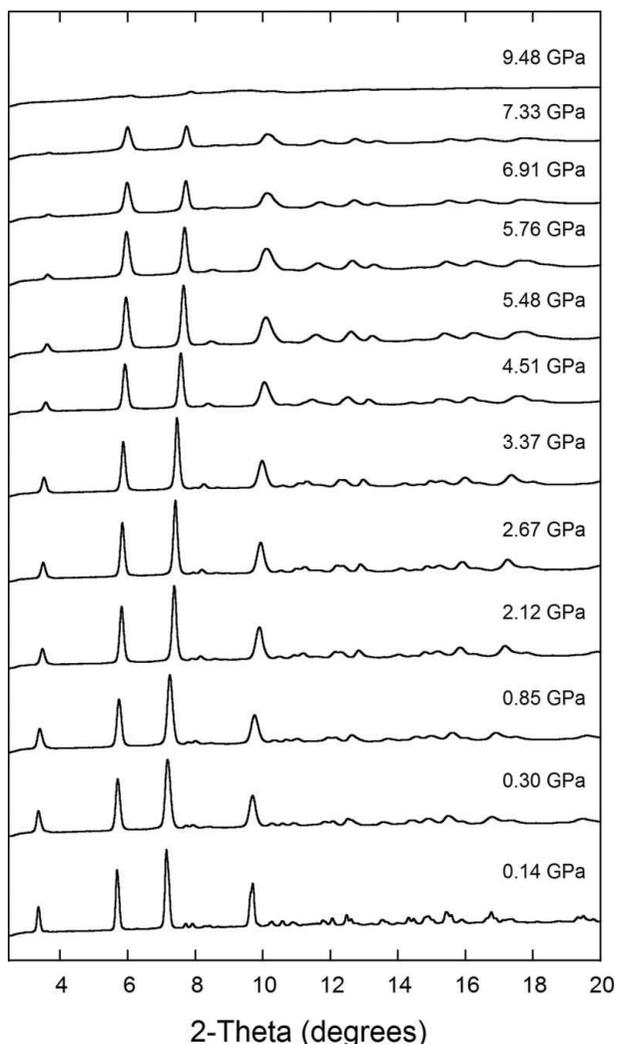
Trobajo, C., Khainakov, S. A., Espina, A. & García, J. R. (2000). *Chem. Mater.* **12**, 1787–1790.

Troup, J. M. & Clearfield, A. (1977). *Inorg. Chem.* **16**, 3311–3314.

Yamamoto, K., Hasegawa, Y. & Nikki, K. (1998). *J. Inclusion Phenom. Mol. Recognit. Chem.* **31**, 289–303.

You, S., Kunz, D., Stöter, M., Kalo, H., Putz, B., Breu, J. & Talyzin, A. V. (2013). *Angew. Chem. Int. Ed.* **52**, 3891–3895.

Zhai, S., Xue, W., Yamazaki, D., Shan, S., Ito, E., Tomioka, N., Shimojuku, A. & Funakoshi, K. (2011). *Phys. Chem. Miner.* **38**, 357–361.